Wear study of structured coated belts in advanced abrasive belt finishing

Kévin Serpin [a,b,*], Sabeur Mezghani [a], Mohamed El Mansori [a]

[a] Arts et Métiers Paris Tech, MSMP — EA 7350, Rue Saint Dominique, BP 508, 51006 Châlons-en-Champagne, Cedex, France
[b] RENAULT S.A.S., Direction de l'Ingénierie de la Production Mécanique, Avenue du Golf, 78280 Guyancourt, France

Keywords:
Belt finishing
Wear
Abrasion
Multiscale analysis

A B S T R A C T

Advanced belt finishing process is remarkably simple and inexpensive. The principle of operation is simple: pressure-locked shoes platens circumferentially press an abrasive coated belt on a rotating workpiece. This abrasive machining process reduces significantly surface irregularities subsequently improving geometrical quality and increasing wear resistance and fatigue life. It is therefore extensively used in automotive industry to superfinish crankshaft journals. However, the major industrial issue about this manufacturing process is its efficiency and robustness.

One of the most promising ways to solve this issue is to control the distribution and morphology of the abrasive grits. Recently a new generation of abrasive belts coated with structured and shaped agglomerate grits has been commercially available. These structured coated belts with mastered cutting edge orientations promise to be more efficient as they have a better wear resistance compared to the traditional coated abrasive belt. Therefore, this work aims to discuss these assumptions and to establish the link between three structured coated belts, the surface finishes and the physical mechanisms which govern their wear performances. In particular a parametric study, based on the cycle time and the rotation speed, is lead in order to analyze the potential of each structure in terms of surface roughness improvement, wear resistance and consumed energy.

The experimental results have demonstrated that, depending on the abrasive structure considered and for a same number of revolutions, modifying the cycle time or the rotation speed can lead to different surface finishes and belt's wear.

1. Introduction

Friction is one of the major issues of mechanical engineering, especially in the automotive engines. One of the ways to reduce friction is to act on surface morphology. In practice, this is achieved either by using anti-friction coating technologies and texturing technology, or in a more traditional way by reducing surfaces roughness with one or multi-step finishing process [1,2].

In a passenger car engine, about 30% of the total frictional loss is accounted by the bearings alone [3]. The process engineering departments working on this key organ have to maintain specific geometrical specifications and very strict surface finishes. In this context, the abrasive belt finishing is surprisingly simple and economical [4]. During the process, pressure-locked shoe-platens circumferentially press an abrasive coated belt on a rotating workpiece. Commonly, this finishing process also includes a low frequency oscillatory movement of the workpiece and belt finishing arm in a direction parallel to the rotations of the workpiece. This abrasive process is used extensively in the automotive industry to superfinish crankshaft journals and pins, which reduces surface irregularities, improves the geometrical quality, and increases wear resistance and fatigue life. However, in practice, belt finishing is a highly complex process.

The performance of this process depends on a large number of variables (grit density, shape and size, oscillations frequency, normal force, contact surface, lubrication fluid type, belts feeding, etc.). It makes its optimization particularly difficult. Moreover, the poor mastery of the active contact area and the abrasive characteristics [4–8] complicate the physical understanding. The crankshaft superfinishing also needs several steps of belt-finishing while successively decreasing the grit size, which involves substantial manufacturing and investments costs. Lastly, the conventional belt finishing machines used in the industry does not ensure sufficiently a good dimensional flexibility and also a change of the diameter of the workpiece necessarily implies a change of the shoes. Several technologies exist to partially solve these issues. Some of them propose to modify the shoes (geometries, material, servo pressure of the inserts), while others change the abrasive belt (grit's morphology, grit's material) or the global kinematic of the apparatus (high oscillations frequency, radial micro-vibration).

In our previous work, we studied, in the same process configuration, the link between grits' morphology, the surface finish of belt-finished workpieces, and the physical mechanisms which govern their wear performance [9]. We found that a coating with slanted grits had the

* Corresponding author at: Arts et Métiers Paris Tech, MSMP — EA 7350, Rue Saint Dominique, BP 508, 51006 Châlons-en-Champagne, Cedex, France.
E-mail address: kevin.serpin@renault.com (K. Serpin).

advantage to ensure a good clipping of roughness profile while preserving valleys depth and thus, preserving the retention capacity of the surface roughness. The belt composed of pyramidal agglomerated grits allowed a very good reducing of the roughness amplitude while having a good wear resistance. Moreover, we saw that dense structures of grits could obstruct the chip's evacuation, generating unpredictable results in terms of roughness. The present study thus aims to extend our previous one by varying the cycle time and the rotation speed.

Nomenclature

t_c	cycle time (s)
N	rotation speed (rpm)
Nr	revolutions number of the sample
Nrc	characteristic revolution number
D	initial workpiece diameter (mm)
R	initial workpiece radius (mm)
L	belt finished width (mm)
R_{pk}	reduced peak height (ISO 13565) (μm)
R_k	core roughness depth (ISO 13565) (μm)
R_{vk}	reduced valley depths (ISO 13565) (μm)
C	circularity (μm)
M_a	multiscale arithmetic roughness average (μm)
MPS	Multiscale Process Signature

2. Experimental procedure

In this work, three abrasive structures are considered. Their behaviors during belt finishing are determined by measuring the surface roughness, the circularity gains, the consumed energy, the belts' wear and the generated chips. An extensive discussion based on physical explanations underlines the behavior of three abrasive structures when the cycle time or the rotation speed increases.

The belt finishing test rig consists of a conventional lathe (power of 9 kW) and a superfinishing apparatus with two machining arms. This leads to a horizontal belt finishing architecture that is usually used for the superfinishing of cylindrical products (ex. crankshafts journals). The abrasive belt is pressed on the journal periphery by two special pressure shoe-platens during a preset cycle-time (Fig. 1).

With this type of shoe-platen, each insert can be moved in a radial direction by hydraulic cylinders that press the abrasive belt against the periphery of the workpiece with a locally known value of contact pressure. One of the benefits of this technology is its flexibility since belts with different thickness can be fit on the shoe-platens without significantly changing the contact surface between inserts and workpiece, which is not the case when traditional shoe-platens with motionless inserts are used. Since the feed pressure of the hydraulic cylinders is the same, a constant pressure distribution is obtained along the abrasive belt/workpiece contact angle (approximately 320°). This pressure value does not change during the process and it can be easily controlled using the feed pressure of cylinders in the shoes.

$$Nr = \frac{tc \times N}{60} \tag{1}$$

The tests were performed in wet conditions varying the abrasive belts structure, the cycle time and the rotation speed, while other working parameters were kept constant (see Table 1). Seven configurations of cycle time/rotation speed were selected and associated to a number of the workpiece's revolutions, calculated with Eq. (1). The experimental design was especially and skillfully built to study the effect of an augmentation of the number of revolutions following two approaches: either by increasing cycle time and keeping constant the rotation speed (cycle time approach), or by keeping constant cycle time and increasing the rotation speed (rotation speed approach). Three types of abrasive belts structures with the same grit's size range (about 30 μm) were considered. There are as follows:

- *Type I:* A common structure often used to superfinish crankshaft journals and pins (see Fig. 2a). The abrasive belt is constituted of a large amount of calibrated grits electrostatically deposited on a polyester backing coated by a layer of synthetic or water based resin. With this deposition process, the grits are oriented perpendicularly to the backing and their cutting edge offers an important material removal capacity. Moreover, this kind of belt can have an anti-slip layer on the backside, which allows for a better hold of the belt during the belt finishing operations.
- *Type II:* A structure composed of lapped grits (see Fig. 2b). The abrasive belt is constituted of grits partially or completely covered by resin. The cutting edges are flattened, well oriented, and less aggressive.
- *Type III:* A shaped structure composed of a plasticized web backing on which pyramidal agglomerates are deposited (see Fig. 2c). Each pyramid has a square base and is constituted of 30 μm grits bound together by a resin. Only the summits are in contact with the workpiece.

The characteristics of the coated abrasive belts used are shown in Table 2. Each configuration was repeated three times. The effects on the belt finishing performances were studied on cylindrical steel samples whose characteristics are given in Table 3. Fig. 3 shows an overview of the workpiece initial surface finish.

Surface roughness profiles and circularities measurements were carried out before and after the tests. The roughness profiles were measured using a 2D Surfascan apparatus. The tip radius of the diamond stylus was 2 μm and the profiles on each specimen were taken along the axial direction over a sampling length of 16.8 mm and at three equally spaced circumferential locations. Circularities were measured by a Mahr MMQ 400 apparatus with a 0.5 mm touch probe. Each journal was measured on three levels: two levels located at 0.5 mm from each

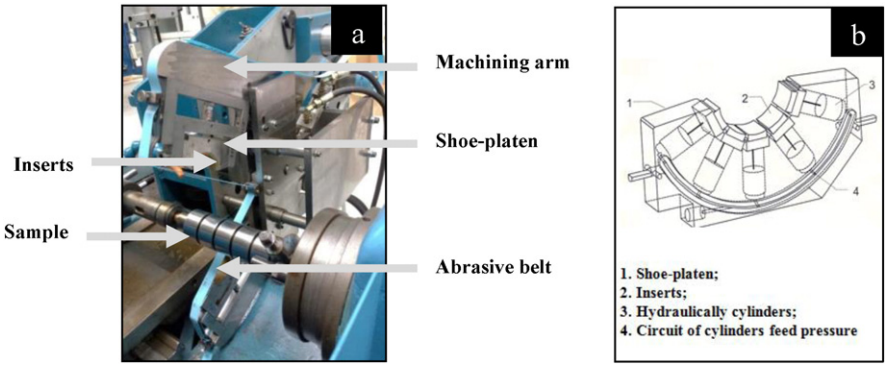

Fig. 1. Belt finishing apparatus (a) and pressure assisted shoe-platen (b).

Table 1
Belt finishing working conditions.

	1	2	3	4	5	6	7
Workpiece rotation speed	100 rpm	100 rpm	100 rpm	100 rpm	200 rpm	400 rpm	800 rpm
Cycle time	12 s	24 s	48 s	96 s	12 s	12 s	12 s
Number of revolution	20	40	80	160	40	80	160
Normal force of the platens	600 N						
Oscillation frequency of shoes	265 cycles/min						
Oscillation amplitude of shoes	1 mm						
Lubrication fluid	Neat oil						
Feed rate of the abrasive belt	None						
Insert hardness	95 Shores						

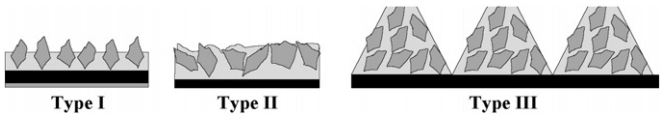

Fig. 2. Three types of abrasive belt structure.

extremity, and one level corresponding to the median plane. The belt-finished surfaces were also measured by a three dimensional white light interferometer (WYKO 3300 NT) in order to complete the topographic analysis.

Furthermore, SEM (JEOL JSM 5510LV) observations of the abrasive belts and chips were performed in order to better understand the combined effect of the belt's type and the cycle time or the rotation speed on the surface. The worn abrasive belts were then cleaned by an ultrasonic bath and the chips were collected via a filter. The belt finishing power has also been recorded, and the average power absorbed during the belt finishing process has been calculated as the average difference between on-load and off-load power.

3. Results and discussions

3.1. Workpiece surface finish

The relative reductions (gain ratio) of the functional roughness parameters Rpk, Rk and Rvk (ISO 13565 standard) were assessed in order to estimate the surface finishing improvements. These parameters are all based on the analysis of the Abbott–Firestone curve (see Fig. 4), which is simply a plot of the cumulative probability distribution of surface roughness height [10].

Rpk, Rk and Rvk are particularly relevant when characterizing textured surfaces since they allow to well describe the roughness profiles' ability in term of friction. Specifically, Rpk is the average height of protruding peaks above the roughness core profile; Rvk is the average depth of valleys projected through roughness core profile; and Rk is the average height of the protruding peaks above the roughness core profile. The workpieces circularity C was also studied. The relative reductions for each parameter were calculated by using Eq. (2), where X can represent Rpk, Rk or Rvk or C.

$$\Delta X(\%) = 100 \times \frac{X^{initial} - X^{final}}{X^{initial}} \quad (2)$$

Table 2
Characteristics of the abrasive belts considered in this study.

Type	Grits size	Model	Supplier	Grits	Backing
I	≈30 μm	372L	3M	Al_2O_3	Polyester
II	≈30 μm	261X	3M	Al_2O_3	Polyester
III	≈30 μm	253FA	3M	Al_2O_3	Web

Results are shown in Figs. 6 and 5. The first two histograms of each graphs are the reference state (tc = 12 s and N = 100 rpm). They show all the impact of the abrasive belts' morphologies on the surface roughness.

We observe that the Type I belt, composed of electrodeposited grits, produces a substantial improvement of the circularity (see Fig. 6) and good roughness peaks and core clipping whatever the configuration tested (see Fig. 5). It should be noted, however, that the Rpk and Rk gain is steady after 40 crankshaft revolutions. This belt also reduces the depth of the roughness valleys, but this time, its effect is strongly dependent on the parameters modified. Indeed, we see that Rvk gain increases with each cycle time while it decreases with rotation speed. Given the large dispersion of Rvk values, this last observation seems to be linked to an unpredictable phenomenon. Finally, these results indicate that this belt is especially relevant for low number of revolutions and rotation speed.

Type II belt has a deeply different behavior. It allows an efficient peak clipping and its effect on roughness core is also substantial (see Fig. 5), whereas the valleys depth is overall preserved, although slightly less deep. Contrary to the previous belt Type I, Type II belt effects increase continuously with the number of revolutions. Moreover, for each number of revolutions, the average effect of Type I belt on roughness parameters does not depend on the process' variables modified. Furthermore, the circularity results are highly dispersed and suggest that it is not improved but preserved (see Fig. 6).

The Type III belt's results follow overall the same trend as the ones of the Type I belt, even if its impact on roughness is lower in comparison. As presented in Fig. 5, its effect on circularity is noticeable, although strongly dispersed. Moreover, by looking at Fig. 6, we can appreciate that its peaks clipping power is hardly influenced by the number of rotation augmentation. Concerning the Rk parameter, it is particularly interesting to see the decrease of the core roughness height with the growth of the rotation speed while it seems to increase with the cycle time. This trend is even stronger on the valleys depth, with a large dispersion when rotation speed increases (as with the Type I belt). Thus, this belt type seems especially devoted for low rotation speed belt finishing.

Finally, we can conclude from surface finish analysis that the cycle time and rotation speed effects on surface roughness are strongly

Table 3
Workpiece characteristics before belt finishing test.

Workpiece material	D38MSV5S Steel (%C 0.35/0.40)
Diameter D	54.8 ± 0.005 mm
Belt finished width L	20 mm (belt width) + 2 mm (oscillations amplitudes)
Fabrication steps	Turning, induction hardening, grinding, 60 μm belt finishing
Superficial hardness	≈55 HRC
Initial roughness	Average Rpk: 0515 μm (±0099 μm) Average Rk: 1964 μm (±0257 μm) Average Rvk: 1449 μm (±0152 μm)

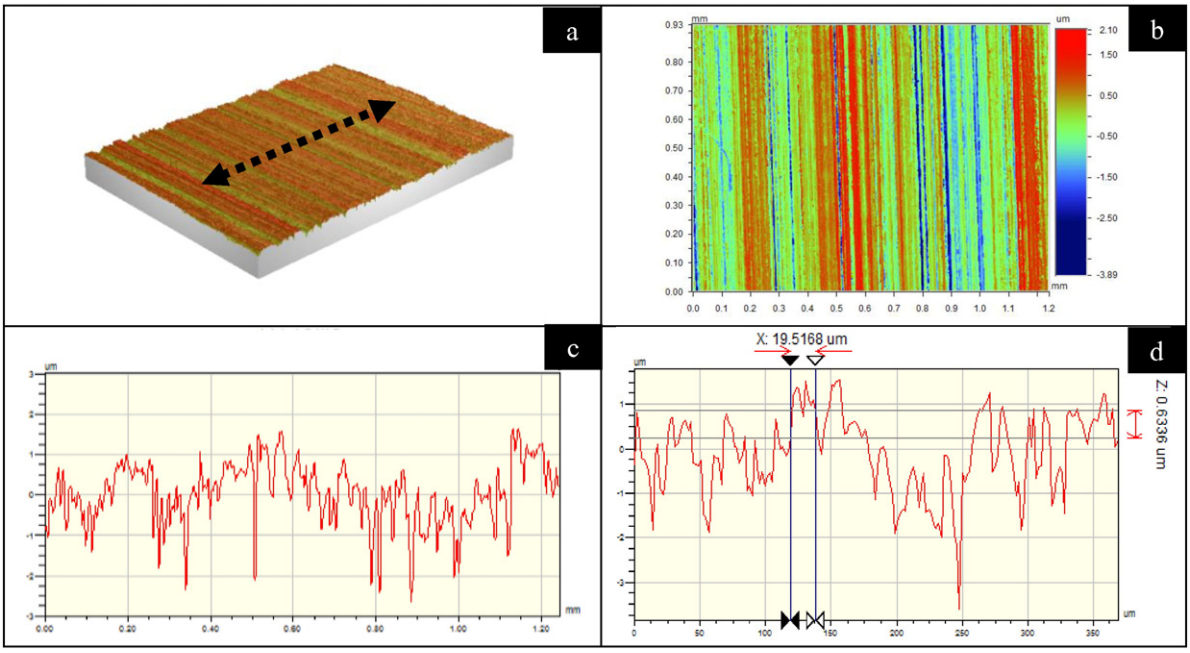

Fig. 3. Initial topology, 3D view (a), 2D view (b) and roughness profiles (c, d).

dependant on the abrasive morphology considered. In particular, one of the major results raised here is that the Type II belt, coated by slanted grits mixed with a resin, clips the roughness peaks and preserves valleys with an effect only dependant on the number of revolutions, whatever the rotation speed and cycle time configuration.

3.2. Multiscale surface finish analysis

In order to quantify more explicitly the effect of each abrasive belt type at all surface finish scales, we investigated the belt finishing process signature on a wide range of scales before and after finishing with the 1D continuous wavelet transformation. To do so, the roughness profiles pass through a filter bank which is a set of contracting wavelets obtained from a unique wavelet function by translation and dilatation. The methodology consists of the extraction of each scale by inversing wavelet transformation, and hence, of the quantification of their arithmetic means values. In fact, the idea is to determine the spectrum of arithmetic mean value from the scales of waviness to roughness M_a [11–13]. This approach allows us to determine the multiscale transfer function of the morphological modification in surface topography after the belt finishing process. This transfer function is denoted as the Multiscale Process Signature (MPS (%)) and is obtained by calculating the M_a gain ratio according to Eq. (3). Here, all the analyses were done by the use of the Morlet wavelet filtering function. Results obtained are shown in Fig. 7.

$$MPS_i(\%) = 100 \times \frac{M_a{}^{initial}(i) - M_a{}^{final}(i)}{M_a{}^{initial}(i)} \quad (3)$$

Overall, we see that each abrasive belt has its own process signature which reflects different abrasion mechanisms [9].

Concerning the Type I belt, we clearly distinguish the effect of the number of revolutions on fine scales. MPS increase with the number of revolutions, whatever the approach considered (cycle time or speed rotation). Furthermore, we see that the potential of MPS improvement is more important when the number of revolution increases by varying the cycle time than varying the rotation speed, which is coherent with the previous results shown in Fig. 6. We also see that the cycle time approach reduces the surface arithmetic roughness up to larger scales than with the rotation speed approach.

By looking at the Type II belt MPS evolution, we immediately see that the arithmetic roughness improvement is lower than those of Type I and Type III. This statement comes from the fact that this arithmetic roughness takes into account only the average of the roughness amplitude in each scale and Type II belt does not remove the deep roughness valleys, as we see in III.1. In addition, the MPS evolution

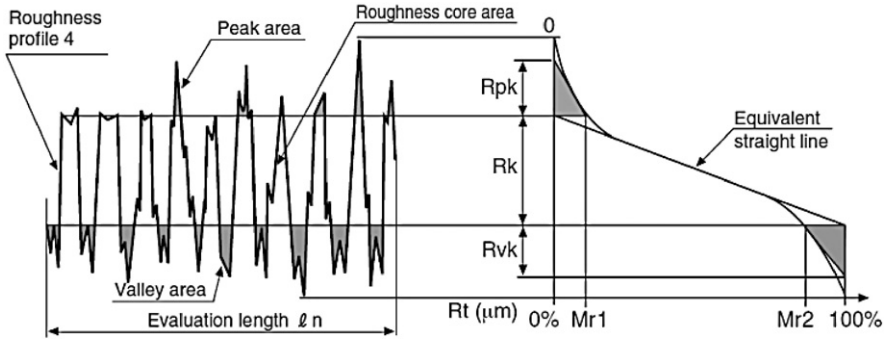

Fig. 4. Abbot–Firestone curve and associated parameters.

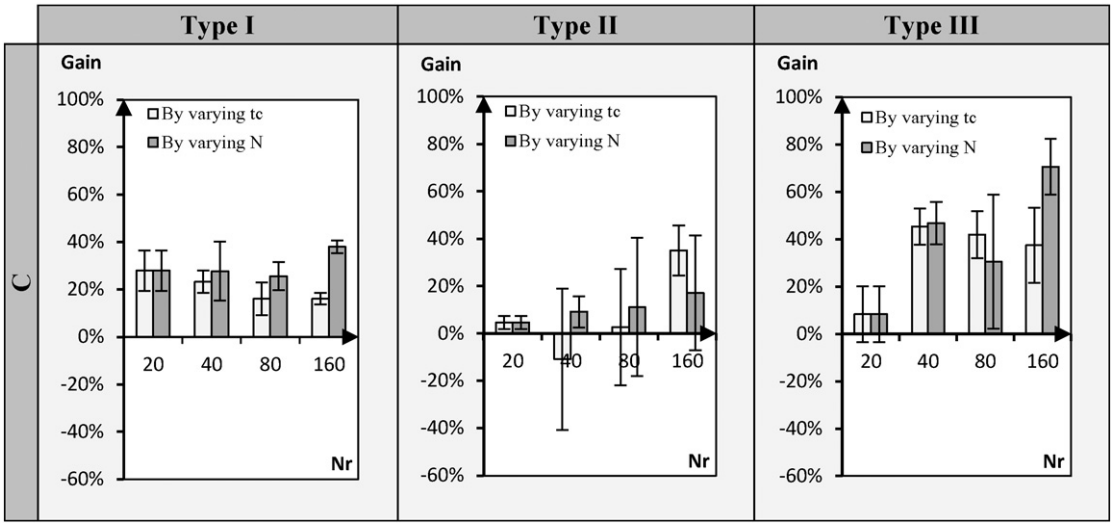

Fig. 5. Circularity relative reduction (gain).

shows that the Type II belt preferentially works on the roughness within the very fine scale. Particularly, we note the presence of a maximum corresponding to the scale of about 18 μm. The analysis of roughness profiles and their associated M_a(see Fig. 3) shows that this value approximately corresponds to the average width of the initial roughness peaks. Furthermore, we also note that the MPS is higher when the number of revolution increases, whatever the approach considered.

The type III belt MPS varies highly with scales. Its level is lower than the Type I belt MPS but greater than the Type II belt one. We can see a maximum within the scales between 0.03 mm and 0.1 mm when the cycle time approach is used. This maximum is greater and greater when cycle time increases, which is again consistent with our previous observations in III.1. In addition, we note that this belt has a small effect within the finest roughness scales. In the largest ones, the MPS is also very low and quickly becomes null to about 1 mm. This observation is even more significant by using the rotation speed approach. Indeed, with this approach, an augmentation of the number of revolution tends to highly deteriorate the MPS and highly reduce the scale size activated during the belt finishing operation.

As we see, this kind of approach and its effect on multiscale roughness strongly interact with the belt's morphology. We particularly retain that the effect of Type II belt on multiscale arithmetic roughness appears independent from the approach, and that increasing the number of rotation reduces the multiscale roughness amplitude, which is in agreement with our conclusion in III.1. This effect is not observed for the others belt's morphologies where great difference appears on MPS in function of the approach considered.

3.3. Abrasive belts' wear and chips characterization

In order to understand these different trends on the roughness of belt-finished workpiece, we have led a SEM analysis of the abrasive belts and chips generated. The idea is to link the abrasive's wear to the chip's shape and the roughness signature observed previously.

By analyzing the worn belts after belt finishing in Fig. 8, we observe that the wear of Type I belts leads to a partial or total loosening of the most prominent grits. This phenomenon depends on the grits characteristics (indentation depth, orientation, cutting edges angle, volume, etc.) and the applied forces. The phenomenon appears most marked for high rotation speed. On the basis of 5 SEM micrographs (magnitude ×200), we count on average 29 breaks/mm^2 at (800 rpm; 12 s) against 15 breaks/mm^2 at (100 rpm; 96 s) and 7 breaks/mm^2 at (100 rpm; 12 s). The number of revolution is thus not sufficient to explain the abrasive wear.

In addition, the chips generated by the micro cut of active grits on the workpieces surface appear mostly well broken. The visible chip's thickness and their lengths vary widely (their thicknesses are ranged from about 1 to 5 μm while their lengths are ranged from several μm to several dozen of μm). No significant overall differences were found between the configurations tested.

The Type II belt's micrograph in Fig. 9 shows a structure with grits partially or completely covered by the resin. The waviness distinguished here corresponds to the underlying grits distribution. Overall the Type I belt's grits offer slanting cutting edges. After belt finishing, abrasion causes an important resin removal and appears flattened. We note the emergence of new cutting edges which initially were totally covered. Furthermore, the grits are well maintained inside the resin since we observe few grit extrusions. There is no noticeable difference between micrographs and at same number of revolution; the wear seems to be similar.

The chips created by this belt are mostly very thin (about 1 μm) and long (several dozens of μm). The chips breaking seems slightly better when the number of revolution increases, particularly at high speed rotation. Moreover, there are few curled chips. Overall, the chips breaking is worse than the Type I one, but there are more uniform.

Finally, the pyramidal shapes of the Type III belt can be observed in Fig. 10. The square base of each pyramid is about 500 μm^2 and the visible size of grits constituting the pyramidal structures is very variable and ranges from few μm to about 30 μm. At low rotation speed and even at great cycle time, this belt resists well to the abrasion. The micrographs show that only the summits had been worn. Thanks to its structure, the abrasion renews the belt's grits by creating new cutting edges and preserves the cutting ability. This belt type thus offers better durability than the Type I classic belts whose grits are quickly broken and where the sharp cutting edges rapidly become rounded. We see that the summits of the pyramidal elements are slightly worn. By contrast with the Type I, this belt's type seems more resistant at high rotation speed. There is no noticeable difference between the belt states at same number of revolution, even at Nr = 160.

The geometrical characteristics of chips are halfway between Type I and Type II ones. Here also, we observe that their thickness and length vary greatly (range from less than 1 to about 5 μm concerning their thickness and range from about 1 μm to about 50 concerning their length). They appear slightly curled and the chips' breaking is worse than with the Type I. No significant overall differences were found between the configurations tested.

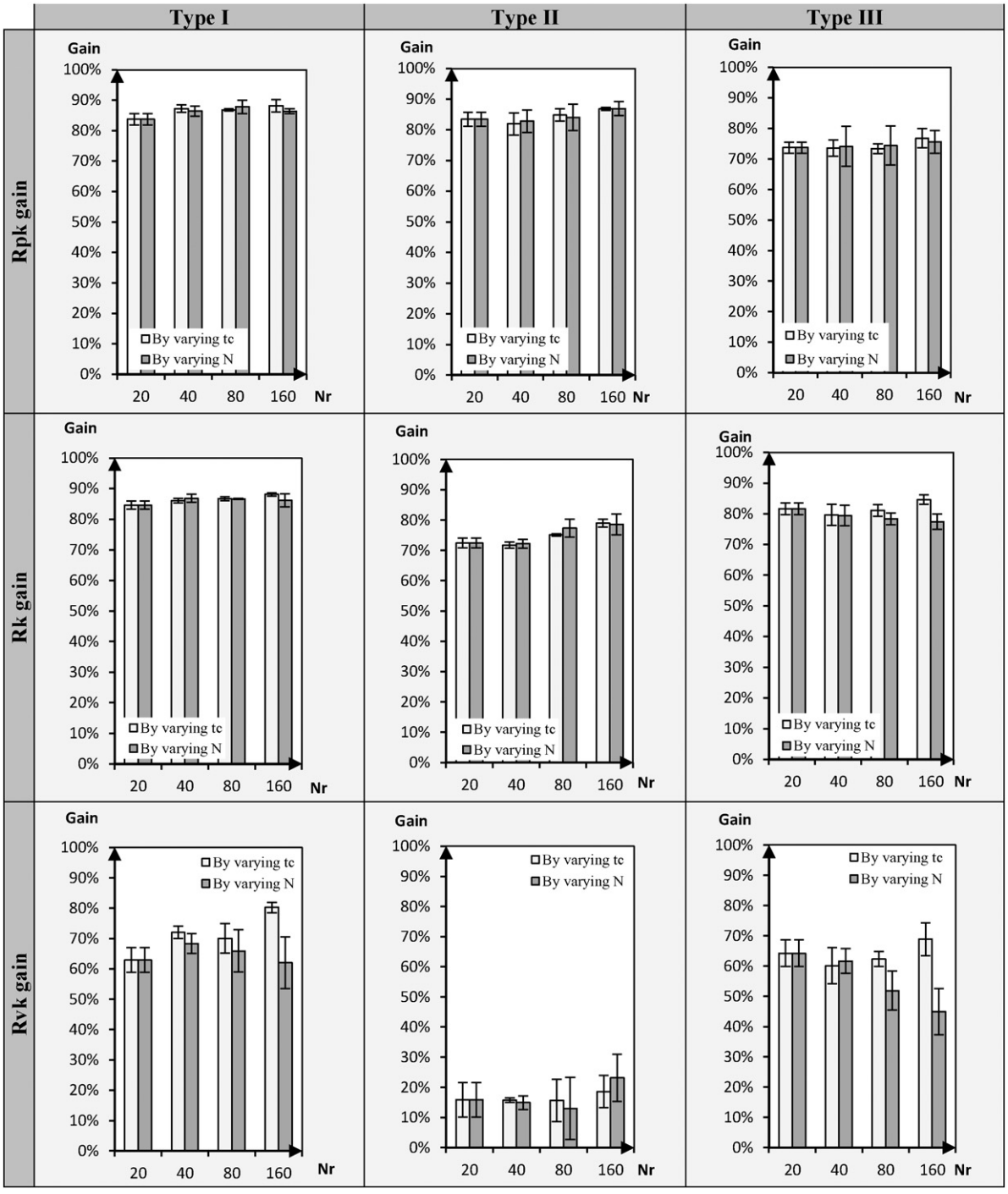

Fig. 6. Roughness relative reduction (gain).

3.4. Consumed energy

In order to complete the analysis and track the evolution of the belt wear, the power was measured and the average consumed energy was calculated every 10 revolutions of the samples. Results given in Figs. 11 and 12 represent the consumed energy in the two extreme belt finishing configurations: the first one at 100 rpm/96 s and the second one at 800 rpm/12 s.

With a cycle time approach, we see that the belt finishing consumed energy coming from the three abrasive morphologies, then decreases and quickly reaches zero. Then after a characteristic number of revolutions, Nrc, the belts' action on surface becomes superficial and surface roughness is not working anymore. The abrasion is stopped. Moreover, we observe that the Type I and Type III abrasives have almost the same Nrc (about 60) while the Type II has the largest one (about 110), about twice as large. Furthermore, this characteristic number corresponds approximately to the number of revolutions where the roughness gain curves begin to differentiate (see Fig. 6).

At the opposite, the belt finishing consumed energies decrease very slightly when speed is very high. It never reaches zero. Moreover, for a same number of revolutions, its values are similar whatever the belt chosen. Thus the abrasion never stops and surface roughness still worked.

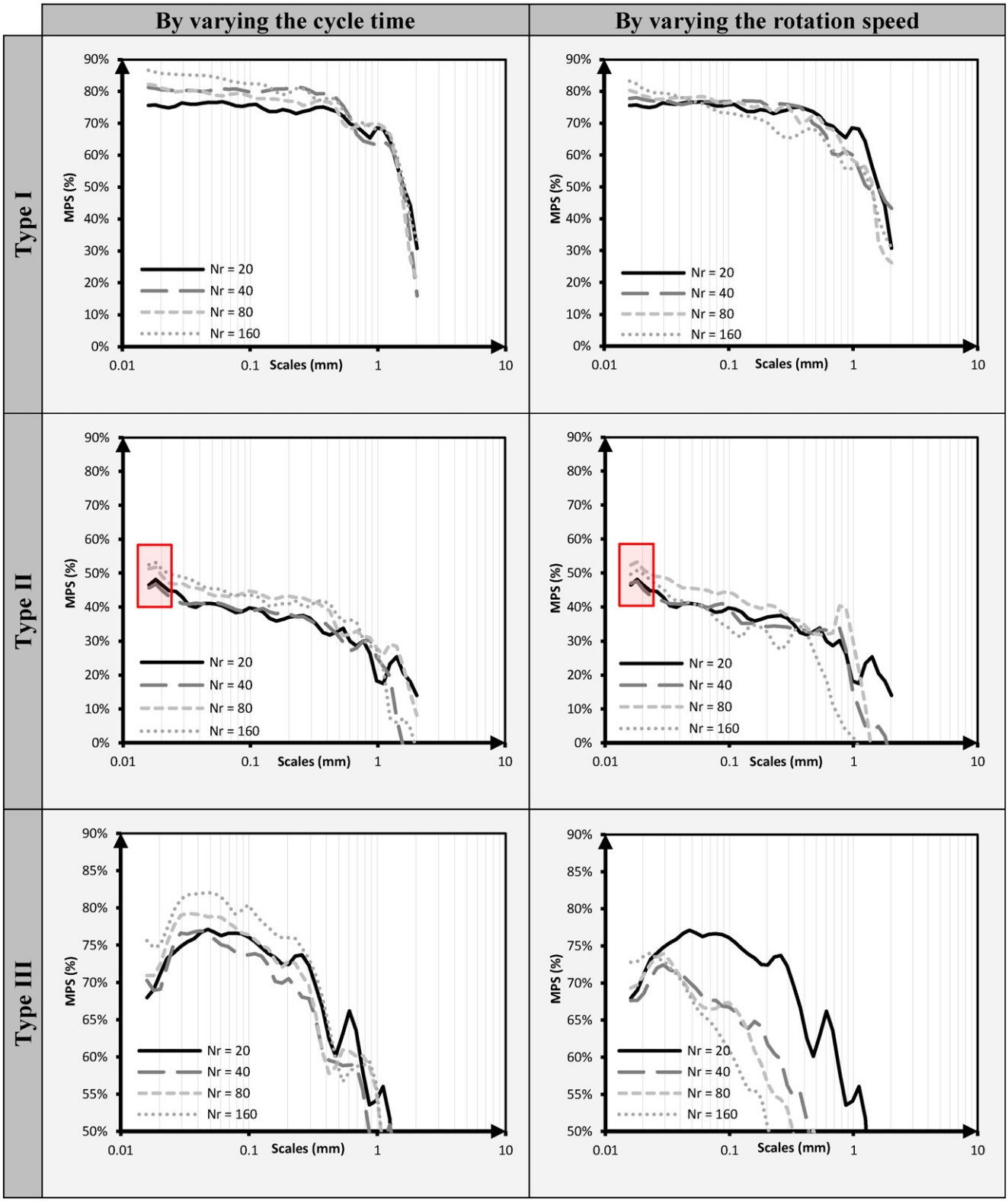

Fig. 7. MPS by varying either the cycle time, either the rotation speed.

3.5. Discussion

We saw here that roughness improvement, wear and consumed energy are strongly dependent on the belt morphology and the activated process variables. The Type II belt has especially a behavior opposite to the Type I and Type III belt ones. At the same number of revolutions, although the energy consumed is widely sensitive to the approach considered, (cycle time or rotation speed) (see Figs. 11 and 12) no effect on the surface roughness is visible (see Figs. 6 and 7). This observation is in accordance with the surface

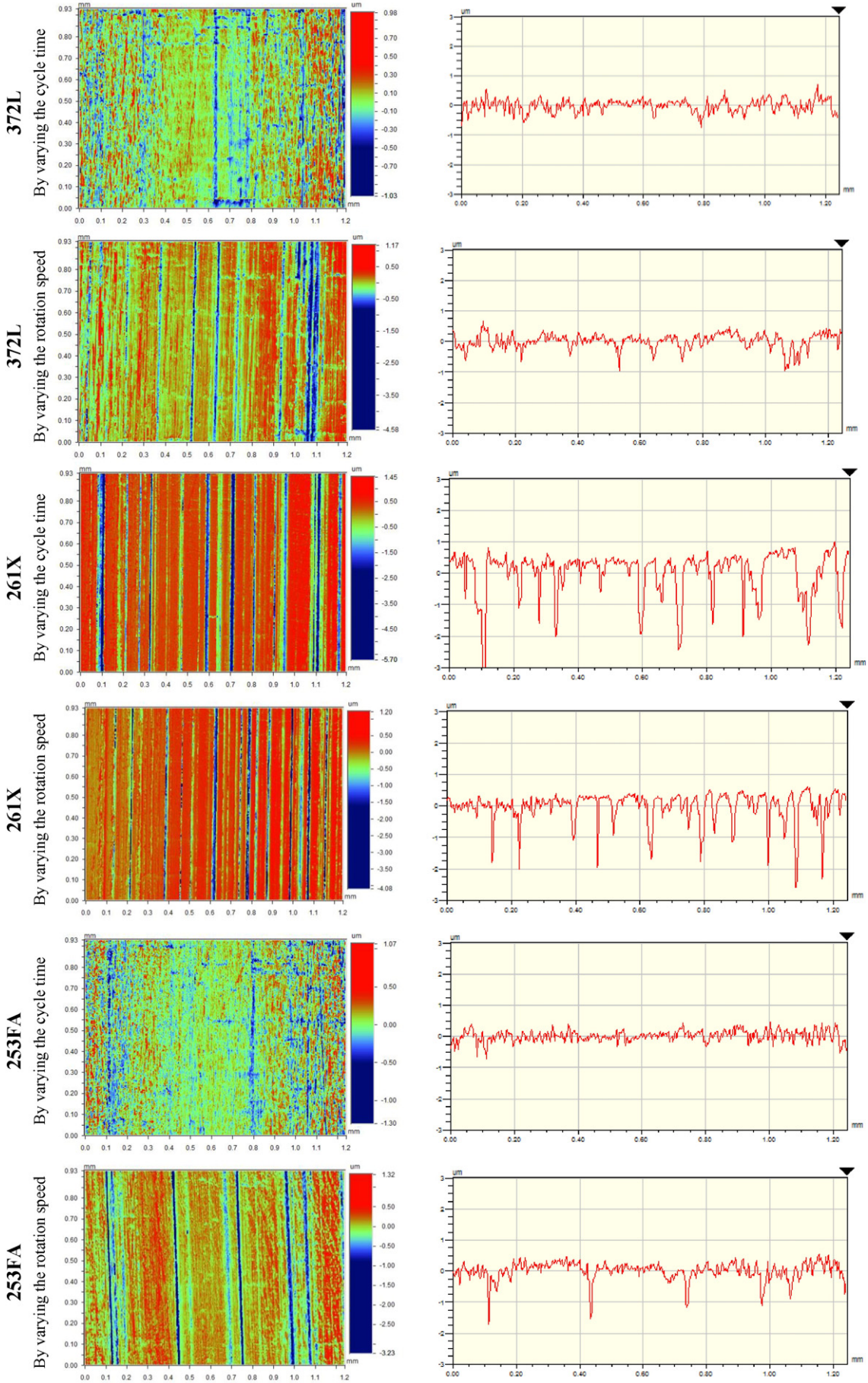

Fig. 8. Topology measurements and roughness profiles at Nr = 160.

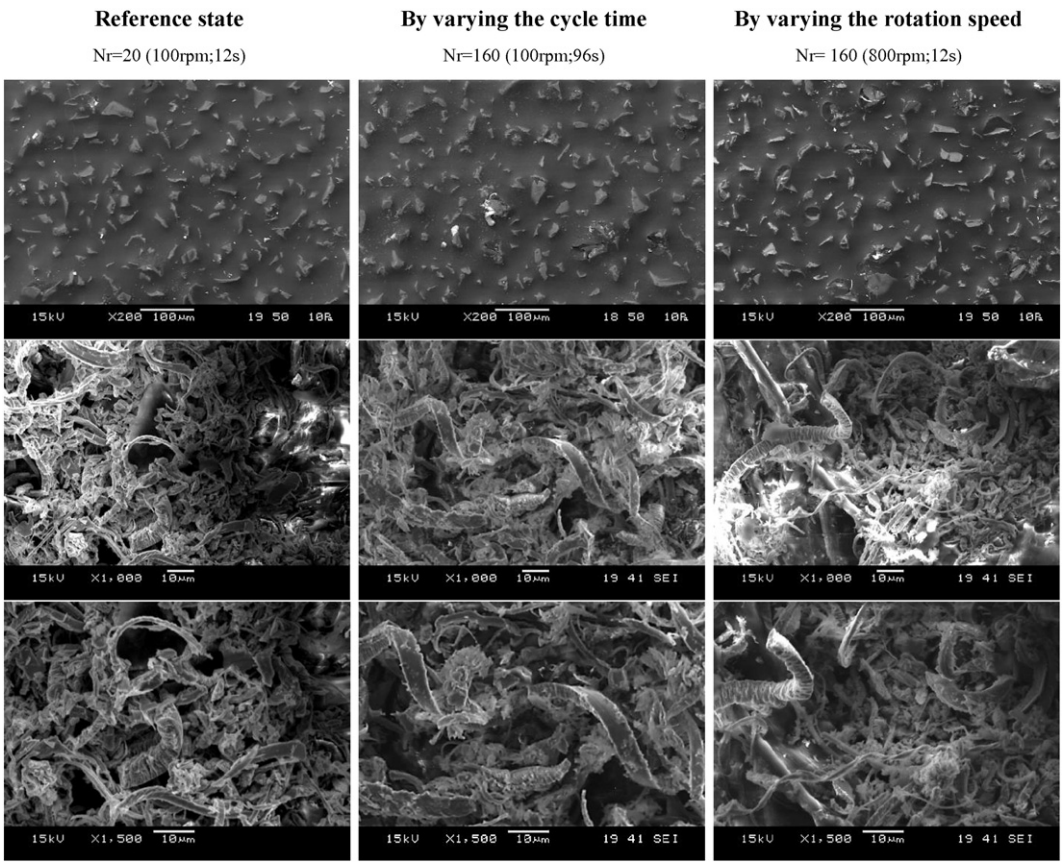

Fig. 9. SEM micrographs showing the Type I belt wear and the generated chips.

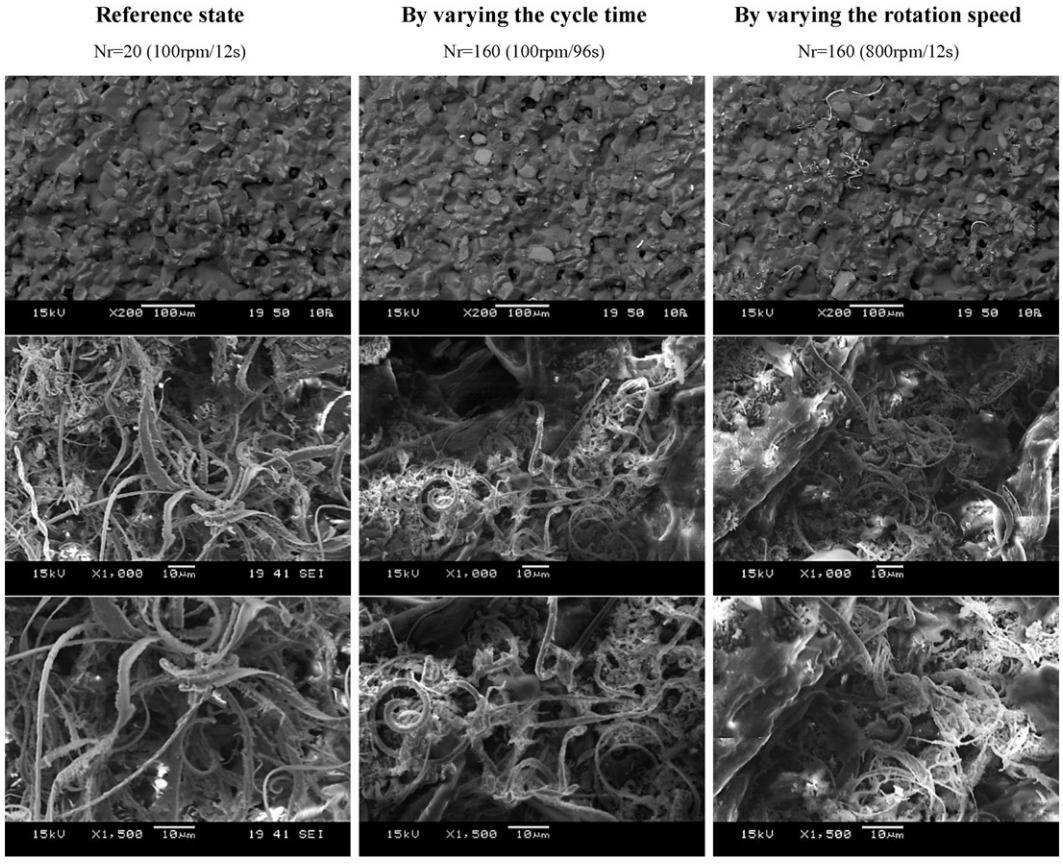

Fig. 10. SEM micrographs showing the Type II belt wear and the generated chips.

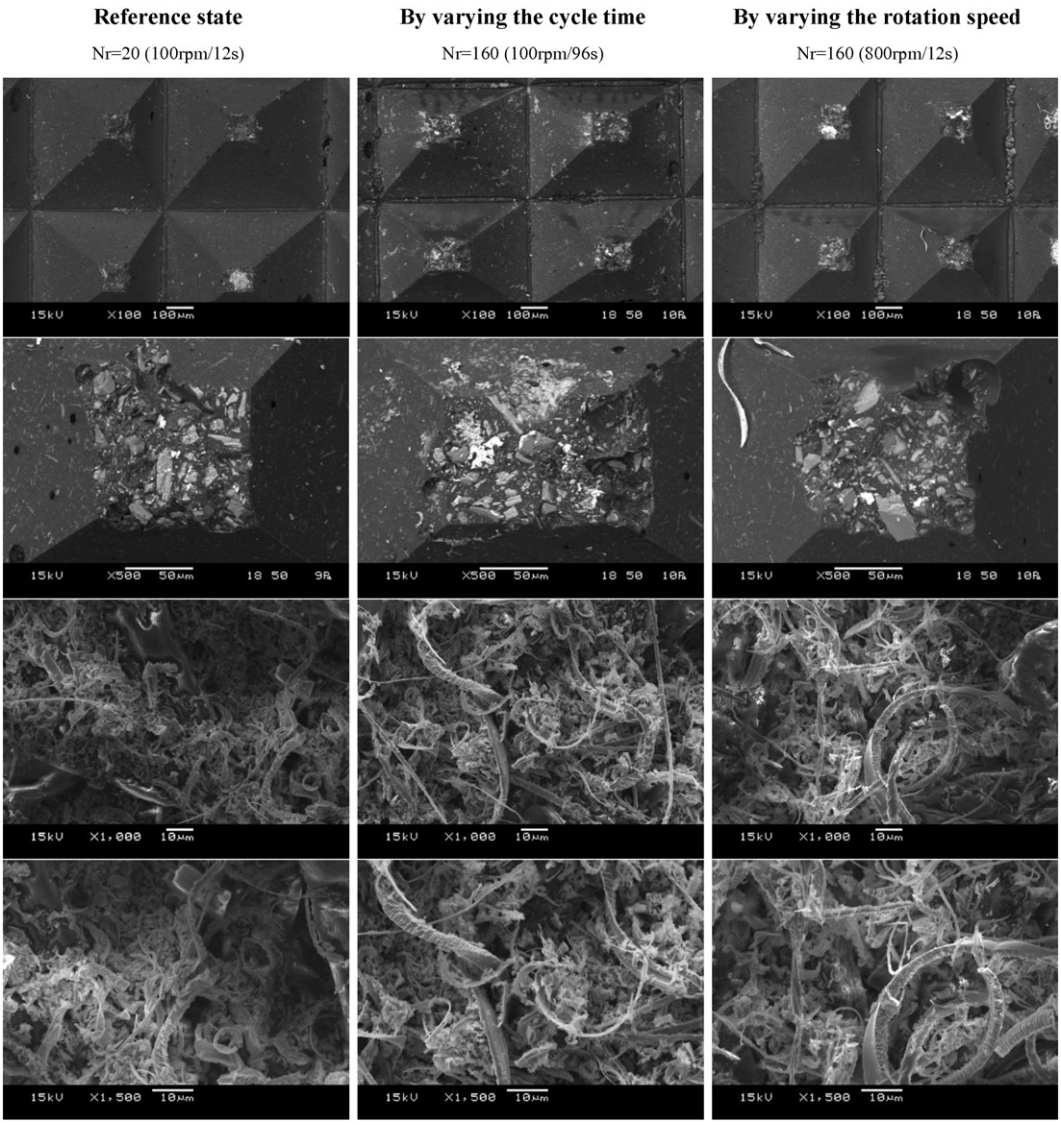

Fig. 11. SEM micrographs showing the Type III belt wear and the generated chips.

topographies obtained by interferometry (see Fig. 8). Actually, several phenomena could potentially explain these trends. We discuss here the two main scenarios:

- Grit's loosening/break

We can reasonably assume that these trends could come from the grits loosening/break. At high rotation speed, the flow of removal material is higher than usual, thus the average mechanical power transmitted from the workpiece to each grit is very significant. Depending on their shapes, sizes and orientations on the belt's backing, cracks can

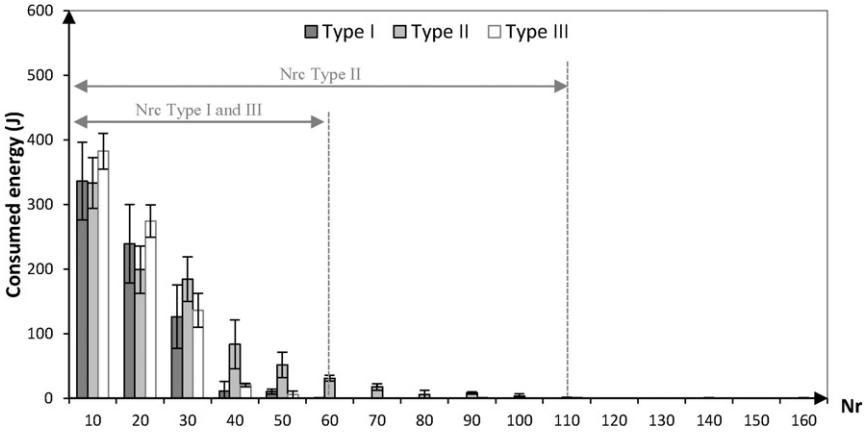

Fig. 12. Average consumed energy every 10 revolutions by varying the cycle time.

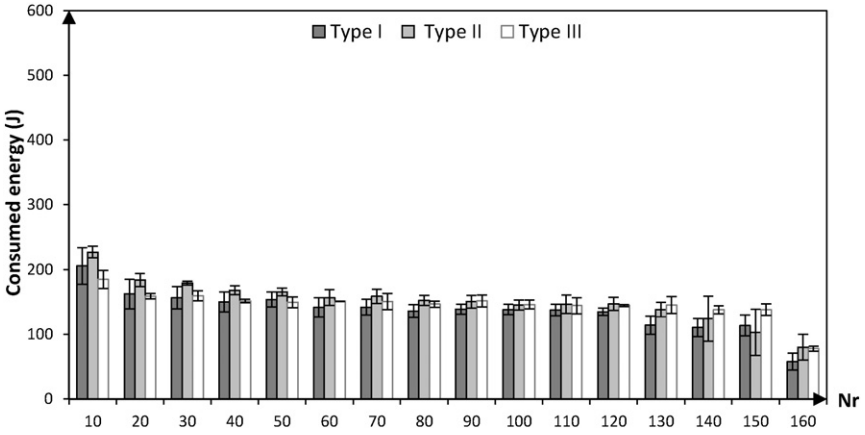

Fig. 13. Average consumed energy every 10 revolutions by varying the rotation speed.

appear inside the grits or develop from the interstice grit/resin, and finally, the break occurs, as see in the SEM observations (see Fig. 8). Because their significant size, these solid debris could be entrapped into the workpiece/belt contact and could produce randomly new very deep valleys. This scenario correlates well with the Type I belt roughness results (see Fig. 6), where the grit's breaks increase indeed with the rotation speed. It could also be applicable to the case of the Type II and III belt, but we did not see any special belt wear at high rotation speed (see Fig. 9). Indeed, at same number of revolutions, the belts state is quite similar. Thus, another phenomenon seems to be behind.

- Centrifugal effect and chips dynamic in the belt/workpiece interstice

Another phenomenon to take into account is the centrifugal effect and the dynamic of the chips evacuation. Depending of the configuration, the chips generated by belt finishing will have more or less ease to evacuate the contact.

At low cycle time and rotation speed, we can hypothesize that the action of the oil flow circulating between the belts and the workpiece surface ensures a partial chips evacuation from the contact. The abrasives structures would not be completely chips saturated and the grits' cutting edges would be partially free. Cutting would be the main mechanism and grits would easily penetrate the workpiece material. The valleys created are deep and pronounced. It can explain why we found that the surface roughness improvements are similar between the two approaches at low cycle time and rotation speed (see Fig. 6).

At high cycle time and low speed rotation, a lot of chips are generated. The oil flow could not ensure anymore the good chips evacuation. Logically, this effect should be more significant when the abrasive structure is rough and dense, which is the case of the Type I and III belts whose the grits are perpendicularly oriented on the backing. The grits' cutting edges of these latter could be quickly covered by chips, thereby deteriorating their indentation ability. This may explain why the ability of these belts is highly modified and why the consumed energy quickly falls and reaches zero after a characteristic time (see Fig. 12). In this condition, the abrasive belt could allow a good clipping of roughness peaks and the valleys generated are less deep. Roughness gain evolutions (see Fig. 6) and topographic observations (see Fig. 8) are fully consistent with this assumption.

Finally, at low cycle time and high rotation speed, the oil flow, affected by the centrifugal force, could ensure a good evacuation of chips from

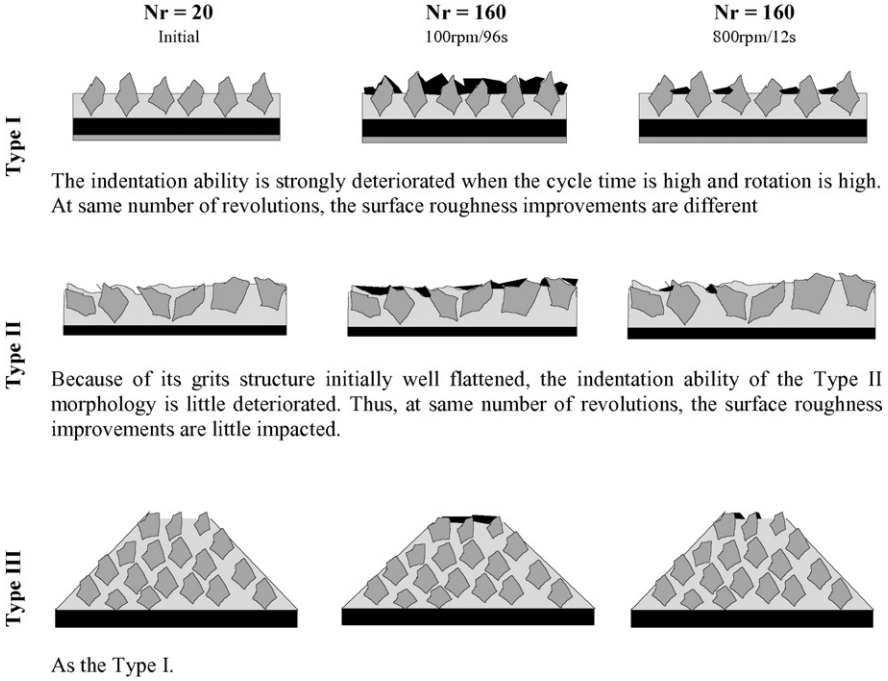

Fig. 14. Effect of the chips saturation depending of the abrasive type.

inside to outside the contact. The space between grits and the cutting edges are then free. The cutting is the main mechanism and the grits indentation ability is maximum. This may clarify why the consumed energy is higher and more consistent than at low speed (see Figs. 12 and 13).

Logically, the higher the initial indentation ability of the abrasive is, the more the effect of the choice of the approach to increase the number of revolution could be significant on the surface roughness improvement. This point is illustrated and commented for each belt type in Fig. 14. Regarding to the results this scenario seems to be the most probable.

4. Conclusions

This paper shows all the effects of the abrasive belts structure during a one step belt finishing. The tests conducted have demonstrated that, at the same number of revolutions, modifying cycle time or rotation speed can lead to a different surface finish, belt's wear, and consumed energy depending on the abrasive morphology considered.

With Type I and III abrasive structures, we see that the number of revolution is not sufficient to explain the roughness modifications and the results follow trends deeply different according to the approach considered (cycle time or rotation speed). More specifically, we saw that the roughness core (Rk) and valleys (Rvk) are the most sensitive and increase with the rotation speed while the roughness peaks (Rpk) are not affected. We observed thanks to the energetic analysis that this effect could find its origin in the chips dynamic associated to the oil circulation. According to this hypothesis, when the speed is low, the chips saturation would quickly occur for a characteristic number of revolutions. At the opposite when the speed is high, the chips saturation would occur very slowly and the abrasion keep acting, even after 160 revolutions. This assumption could explain why the indentation ability appears particularly impacted by a change of approach. In all cases, the Type II belt is the less sensitive. It is thus particularly attractive. It enables to improve roughness quality (mainly peaks and core height) and/or reduce cycle time simply by increasing the rotation speed.

References

[1] M. El Mansori, E. Sura, P. Ghidossi, S. Deblaise, T. Dal, H. Khanfir, Toward physical description of form and finish performance in dry belt finishing process by a tribo-energetic approach, J. Mater. Process. Technol. 182 (2007) 498–511, http://dx.doi.org/10.1016/j.jmatprotec.2006.09.009.

[2] M. Bigerelle, B. Hagege, M. El, Mechanical modelling of micro-scale abrasion in superfinish belt grinding, Tribol. Int. 41 (2008) 992–1001, http://dx.doi.org/10.1016/j.triboint.2008.03.015.

[3] K. Holmberg, P. Andersson, A. Erdemir, Global energy consumption due to friction in passenger cars, Tribol. Int. 47 (2012) 221–234, http://dx.doi.org/10.1016/j.triboint.2011.11.022.

[4] M.C. Shaw, Principles of Abrasive Processing, Oxford Science Publications, Clarendon Press, Oxford, 1996.

[5] M.C. Shaw, Fundamentals of the grinding process, Proceedings of the International Grinding Conference, Carnegie Press, Pittsburgh, PA 1972, pp. 220–258.

[6] W.R. Backer, E.R. Marshall, M.C. Shaw, The size effect in metal cutting, Trans. ASME. 74 (1952) 61–72.

[7] M.C. Shaw, D.A. Farmer, K. Nakayama, Mechanics of the abrasive cut-off operation, Trans. ASME J. Eng. Ind. 89 (1967) 495–502.

[8] Z.B. Hou, R. Komanduri, On the mechanics of the grinding process — part I, Stoch. Nat. Grind. Process 43 (2003) 1579–1593, http://dx.doi.org/10.1016/S0890-6955(03)00186-X.

[9] K. Serpin, S. Mezghani, M. El Mansori, Multiscale Assessment of Structured Coated Abrasive Grits in Belt Finishing Process, Wear, 2015.

[10] L. De Chiffre, P. Lonardo, H. Trumpold, D.A. Lucca, G. Goch, C.A. Brown, et al., Quantitative characterisation of surface texture, CIRP Ann. - Manuf. Technol. 49 (2000) 635–652.

[11] L. Sabri, S. Mezghani, M. El Mansori, H. Zahouani, Multiscale study of finish-honing process in mass production of cylinder liner, Wear 271 (2011) 509–513, http://dx.doi.org/10.1016/j.wear.2010.03.026.

[12] S. Mezghani, M. El, A. Massaq, P. Ghidossi, Correlation between surface topography and tribological mechanisms of the belt-finishing process using multiscale finishing process signature, C. R. Mecanique. 336 (2008) 794–799, http://dx.doi.org/10.1016/j.crme.2008.09.002.

[13] M. El Mansori, S. Mezghani, L. Sabri, H. Zahouani, On concept of process signature in analysis of multistage surface formation, Surf. Eng. 26 (2010) 216–223.